

# Discrete sampling of extreme events modifies their statistics

Lior Zarfaty,<sup>1</sup> Eli Barkai,<sup>1</sup> and David A. Kessler<sup>2</sup>

<sup>1</sup>*Department of Physics, Institute of Nanotechnology and Advanced Materials, Bar-Ilan University, Ramat-Gan 52900, Israel*

<sup>2</sup>*Department of Physics, Bar-Ilan University, Ramat-Gan 52900, Israel*

We explore the extreme value (EV) statistics of correlated random variables modeled via Langevin equations. Starting with an Ornstein-Uhlenbeck process, we find that when the trajectory is sampled discretely, long measurement times make the EV distribution converge to that originating from independent and identically distributed variables drawn from the process' equilibrium measure. A transition occurs when the sampling interval vanishes, for which case the EV statistics corresponds to that of the continuous process. We expand these findings to general potential fields, revealing that processes with a force that diminishes for large distances exhibit an opposite trend. Hence, we unveil a second transition, this time with respect to the potential's behavior at large displacements.

Extreme value (EV) statistics is a venerable branch of probability theory, and has drawn much interest over the years [1, 2]. It finds diverse applications, from physics of nonequilibrium dynamics [3], to analysis of the fastest times for biological processes like fertilization [4], to geological data such as the rate of large earthquakes [5], and on to applications of risk management in finance [6], to name a few. The theory that deals with EV statistics of a set of independent and identically distributed (IID) random variables (RV) is in itself a classical problem [7, 8]. However, for natural phenomena correlations are omnipresent, and studying EV statistics in their presence still remains a challenging field [9–12].

One of the most well-known examples of a correlated trajectory is that of a Brownian particle in a force field. Here, at least theoretically, one may envision two approaches. In the first we search for the maximum of the path in a certain time window, and in the second we first discretely sample (DS) the path and then find the maximum of the sampled data. Since any experimental study cannot collect an infinite amount of data, the discrete sampling approach is clearly more related to real world applications. Is there a major difference between the two methods?

Naively, if the time between sampling events is shorter than the correlation time of the process, and assuming correlations decay exponentially (we rule out exotic anomalous processes), then the sampling time should not be expected to play a major role. However, as we show here, for a very wide class of Langevin processes, where the restoring force is strong enough (see below) and for any finite sampling time, this is wrong. The consequence is that as we increase the measurement time we may witness a qualitative transition in the statistics of extremes, which is not related to a physical change of the system. The remarkable aspects of our study is the non-smooth transition that takes place between discrete and continuous sampling (CS), which is surprisingly found when the time between samplings approaches zero, and a second transition governed by the large-displacement behavior of the force field controlling the dynamics. Technically, these observations are related to the fact that discretely

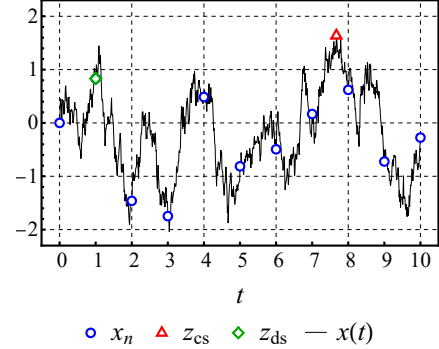


FIG. 1. (Color online) The trajectory of a Brownian particle in a confining harmonic force, modeled via the OU process. The maximum of this path is  $z_{cs}$  (marked by the red triangle), while for DS every  $\Delta = 1$  units of time, yielding the sequence  $x_n$  (blue circles), the maximum is  $z_{ds}$  (green diamond).

sampled systems are described by an integro-differential master equation, while the commonly studied CS approach [11] employs the Fokker-Planck equation. As we shall show, the latter description can break down at large times.

We start by considering the Langevin equation,

$$\frac{d}{dt}x(t) = \frac{1}{\tau}F[x(t)] + \sqrt{2D}\eta(t), \quad (1)$$

where  $\tau$ ,  $D$ , and  $\eta(t)$  are the relaxation time, the diffusion coefficient, and the standard Gaussian white noise, respectively. The noise obeys  $\langle \eta(t)\eta(t') \rangle = \delta(t-t')$  and has zero mean, where  $\delta(\cdot)$  is Dirac's delta function. The path  $x(t)$  is subjected to a force  $F(x) = -dU(x)/dx$ , where  $U(x)$  is the potential. We rescale the equation such that  $t[x(t)]$  is measured in units of  $\tau[\sqrt{D\tau}]$ . The model Eq. (1) with  $U(x) = x^2/2$  is the Ornstein-Uhlenbeck (OU) process, describing the motion of an overdamped particle in an harmonic field or, equivalently, the velocity of an underdamped Brownian particle.

We specialize to this OU process path  $x(t)$  in the time interval  $[0, T]$ , and sample it stroboscopically every  $\Delta$  units of time, see Fig. 1. The outcome of this DS measurement is the random sequence  $x_n \equiv x(n\Delta)$ , where

$0 \leq n \leq N$  and  $N\Delta = T$  is the total measurement time. We focus on the maximum of this set, denoted  $z_{\text{ds}}$ , and compare its properties to those of the previously studied case of the maximum of  $x(t)$  in the interval  $[0, T]$ ,  $z_{\text{cs}} \equiv \max_{0 \leq t \leq T} [x(t)]$  [11]. To compute this latter quantity, one has to measure the whole continuous trajectory and hence we call it the CS model. Clearly,  $z_{\text{ds}} \leq z_{\text{cs}}$ .

The binding force ensures that an ensemble of particles will reach a steady state, the Boltzmann-Gibbs measure, given by  $\exp[-U(x)]/Z$  where  $Z \equiv \int_{-\infty}^{\infty} dx \exp[-U(x)]$  is the partition function (for the OU process  $Z = \sqrt{2\pi}$ ). In the limit of large  $\Delta$  and  $T$  but fixed  $N$ , the sampling is of uncorrelated RVs all drawn from the equilibrium density. In this case, we can use the fact that if  $z_{\text{ds}} < z$  then all the  $N$  sampled variables are also smaller than  $z$ , and since they are IID we find

$$\lim_{\Delta \rightarrow \infty} \text{Prob}(z_{\text{ds}} < z) = \left[ \int_{-\infty}^z dx \frac{e^{-U(x)}}{Z} \right]^N. \quad (2)$$

It will prove useful to rewrite this as  $\text{Prob}_{\text{iid}}(z_{\text{ds}} < z) = \exp[-N \ln[1/\Lambda_{\text{iid}}(z)]]$ . In this limit, the nature of the EV statistics is due to the equilibrium properties of the system only, and dynamical information such as the correlation effects is wiped out. Note that when  $N$  is large the EV is also large [13], hence we focus on the limit  $z \gg 1$ . In this case  $\Lambda_{\text{iid}}(z) \simeq 1 - [U'(z)]^{\alpha_{\text{iid}}} \exp[-U(z)]/Z$ , with  $\alpha_{\text{iid}} = -1$ . This simple result is general and goes beyond the case of the OU process.

To treat the EV problem, we consider the path's values at the moments of sampling  $x_n$  using a discrete stochastic map. Integrating the Langevin equation Eq. (1), we find  $x_{n+1} = \mu x_n + \sqrt{1 - \mu^2} \eta_n$ , where  $\eta_n$  is a standard Gaussian deviate and  $\mu = \exp(-\Delta)$ . In the large  $N$  limit, we find

$$\text{Prob}(z_{\text{ds}} < z) \sim A(z) \exp \left\{ -N \ln \left[ \frac{1}{\Lambda_*(z)} \right] \right\}. \quad (3)$$

The amplitude  $A(z)$  approaches unity for large  $z$  and the main focus here is the ground-state eigenvalue  $\Lambda_*(z)$ . The latter obeys the following integral equation, obtained from the stochastic map,

$$\Lambda_*(z) P_*(x; z) = \int_{-\infty}^z \frac{dx' P_*(x'; z)}{\sqrt{2\pi(1 - \mu^2)}} \exp \left[ -\frac{(x - \mu x')^2}{2(1 - \mu^2)} \right], \quad (4)$$

where  $P_*(x; z)$  is the corresponding ground-state eigenfunction (since  $N$  is large we consider here the smallest eigenvalue). Studying the joint limit of  $\Delta \rightarrow 0$  and  $N \rightarrow \infty$  with  $T$  fixed and large, we obtain the Fokker-Planck description of the problem corresponding to the CS case,

$$\begin{aligned} \Lambda_*(z) &\simeq \Lambda_{\text{cs}}(z) \equiv 1 - \Delta \lambda_{\text{cs}}(z) \\ &\simeq 1 - \Delta [U'(z)]^{\alpha_{\text{cs}}} \frac{e^{-U(z)}}{Z}, \end{aligned} \quad (5)$$

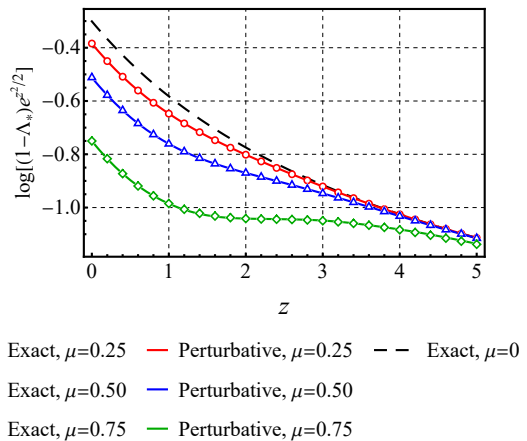


FIG. 2. (Color online) The scaled ground-state eigenvalue  $(1 - \Lambda_*) \exp(z^2/2)$  for  $\mu = 0.25$  (marked by red circles),  $0.5$  (blue triangles), and  $0.75$  (green diamonds), obtained from numerical evaluations [17] of the eigenvalue equation, Eq. (4), as well as from a 10th-order expansion in  $\mu$  (solid curves). Also shown is the exact result for the IID case,  $\mu = 0$ , for which  $\Lambda_{\text{iid}}(z) = \Phi(z)$  (dashed line). Note that all three finite- $\mu$  curves merge for large  $z$  with the IID curve.

where  $\alpha_{\text{cs}} = 1$  [Eq. (5) is actually valid for any  $U$ ] [14]. It was shown in Ref. [11] that for the OU case,  $\lambda_{\text{cs}}(z)$  is the solution of  $D_{\lambda_{\text{cs}}^{\text{ou}}(z)}(-z) = 0$ , where  $D_{\cdot}(\cdot)$  is the parabolic cylinder function. We note that the large- $z$  asymptotics of  $\lambda_{\text{cs}}^{\text{ou}}(z)$  is recovered by our Eq. (5) [15]. Our major result is that the limit of  $\Delta \rightarrow 0$  is singular in the context of EV theory, as for any finite  $\Delta$ , the large-time limits of the two approaches, DS (integral equation) and CS (Fokker-Planck), are significantly different, both for the OU process along with a wide class of similar processes.

To begin analyzing the DS problem, we use a small- $\mu$  perturbation theory, expanding  $\Lambda_*(z) = \sum_{n=0}^{\infty} \lambda_n(z) \mu^n$ , and similarly for  $P_*(x; z)$ . Using Eq. (4), we get to first order in  $\mu$  that  $\Lambda_*(z) \simeq \Phi(z) + \mu \exp(-z^2)/[2\pi\Phi(z)]$ , with  $\Phi(z) \equiv [1 + \text{erf}(z/\sqrt{2})]/2$  (note that this is the integrated equilibrium measure). For large- $z$  this implies that

$$\Lambda_*(z) \simeq 1 - \frac{e^{-z^2/2}}{\sqrt{2\pi}z} + \mu \frac{e^{-z^2}}{2\pi}. \quad (6)$$

The leading-order term is expected as it is the result obtained for IID RVs drawn from the equilibrium density. The key observation is that for large  $z$ , the correction term is by far smaller than the leading order, even if  $\mu$  is not too small, since  $\exp(-z^2/2) \ll 1$ . Surprisingly, a similar result is valid for the correction term *generally* (for any  $U$ ) [14]. Namely, the first-order correction with  $\mu$  is exponentially small in  $z$  with respect to the leading term. We continue the small- $\mu$  expansion to order 20 [16] and find similarly, that all the terms up to  $\mu^{20}$  are negligible in the large- $z$  limit. This behavior is also found in numerical calculations of the eigenvalue  $\Lambda_*(z)$  [17], as exhibited in Fig. 2, showing that for large values of  $z$  all

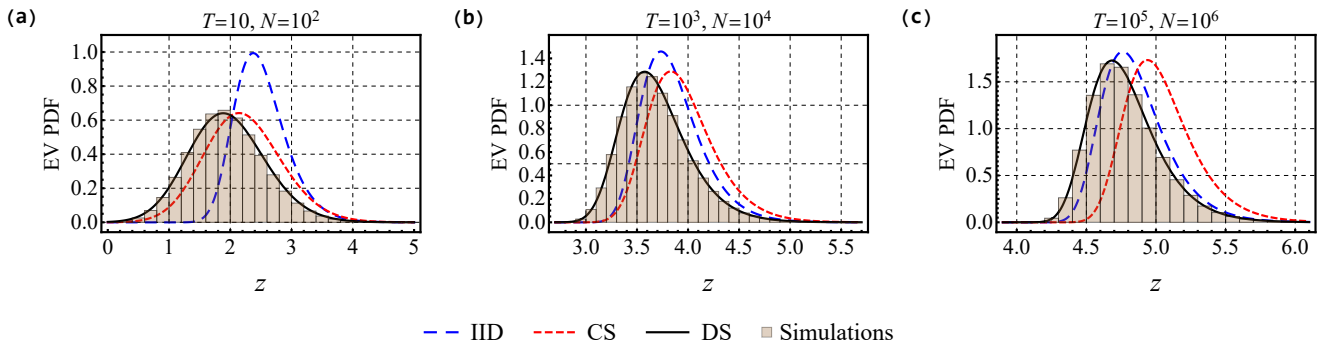


FIG. 3. (Color online) The distribution of EVs for the DS OU process, with  $\Delta = 0.1$ . For not too large  $T$ , we see a behavior close to that of the CS approach, see panel (a). However, as we increase  $T$ , approximating the DS statistics by those of CS becomes less accurate, see panel (b), and eventually approaches the statistics predicted for  $N = T/\Delta$  IID RVs drawn from equilibrium, see panel (c). The IID and DS curves (dashed blue and solid black) correspond to  $\exp\{-N \ln[1/\Lambda(z)]\}$  with  $\Lambda(z) = \Phi(z)$  and  $\Lambda(z) = \Lambda_*(z)$  [17], respectively. The CS curve (short-dashed red) corresponds to  $\exp[-T\lambda_{cs}^{ou}(z)]$ , where  $D_{\lambda_{cs}^{ou}}(-z) = 0$ . Each histogram is made of  $10^6$  maxima whose initial conditions are  $x = 0$ , evolving via the stochastic map  $x_{n+1} = \mu x_n + \sqrt{1 - \mu^2} \eta_n$ .

the numerical data converge to a unique curve which is  $\Delta$  independent, namely the IID curve. This, as a starting point, suggests that when  $z$  is large the EV statistics will converge to that of uncorrelated RVs drawn from the equilibrium density for any finite  $\Delta$ .

To further explore the EV theory at large  $z$ , we need a third strategy using the large- $z$  expansion of the integral equation, Eq. (4) [17]. Expressing the ground-state eigenvalue as  $\Lambda_*(z) \simeq 1 + \exp(-z^2/2)\Lambda_1(z) + \exp(-z^2)\Lambda_2(z)$ , and similarly for  $P_*(x; z)$ , we obtain

$$\Lambda_*(z) \simeq 1 + e^{-z^2/2} \underbrace{\left[ -\frac{1}{2} e^{z^2/2} \text{erfc}\left(\frac{z}{\sqrt{2}}\right) \right]}_{\Lambda_1(z)} + e^{-z^2} \underbrace{\frac{1}{2\pi} \sum_{n=1}^{\infty} \frac{\mu^n/n!}{1 - \mu^n} \text{He}_{n-1}^2(z)}_{\Lambda_2(z)}, \quad (7)$$

where  $\text{He}_n(\cdot)$  is the  $n$ th probabilist's Hermite polynomial and  $\text{erfc}(\cdot)$  is the complementary error function. Further expanding the expression for large- $z$ , we find

$$\Lambda_*(z) \simeq 1 - \frac{e^{-z^2/2}}{\sqrt{2\pi}z} + \frac{(1 + \mu)^2 e^{-z^2/(1+\mu)}}{2\pi z^2 \sqrt{1 - \mu^2}} \simeq 1 - \frac{e^{-z^2/2}}{\sqrt{2\pi}z} \left( 1 - \frac{2e^{-\Delta z^2/4}}{z\sqrt{\pi\Delta}} \right), \quad (8)$$

where the last expression is for small  $\Delta$ . Remarkably, the leading two terms are  $\mu$  independent and correspond to the result for IID variables drawn from equilibrium density. However, when  $\Delta$  becomes small, or equivalently  $\mu$  approaches unity, the last term becomes equally important, indicating the existence of a crossover regime to a CS behavior for  $\Delta z^2 \sim \mathcal{O}(1)$ . This is evidenced in Fig. 3, where one sees that for small  $T = \Delta N$ , the PDF of  $z_{ds}$  is

close to the CS prediction, whereas for large  $T$  it appears to converge to the IID limit. This transition has however nothing to do with a physical switch of the behavior of the system, and is rather a purely statistical effect due to the finite sampling rate. Thus, for any fixed  $\Delta > 0$ , as  $T$  becomes large the IID statistics and the equilibrium measure take control of the EV theory.

We now present a simple explanation to this result. Consider the maximum of the correlated sequence  $x_n$ , and reshuffle randomly all the data. After reshuffling we remain with no correlation, but the maximum of the reshuffled data is still clearly the same as the maximum of the non-reshuffled data set. Further in the reshuffled data set, we have IID RVs drawn from the Boltzmann-Gibbs equilibrium measure. Thus, it is obvious that we get an IID-like behavior for the EVs. But why does this reasoning break down for small  $\Delta$ , and how are we to understand the origin of the crossover scale  $\Delta z^2 \sim \mathcal{O}(1)$ ? Expanding the recursion relation of  $x_n$  for small  $\Delta$ ,  $x_{n+1} - x_n \simeq -\Delta x_n + \sqrt{2\Delta} \eta_n$ , we see that there is a competition between two terms. For small  $\Delta$  the stochastic noise is dominant, and so a record-breaking large  $x_n$  is very liable to be followed by a yet larger value. However, for sufficiently large  $x_n$ , the deterministic term which is proportional to  $x_n$  dominates, so those maxima are separated by large gaps in time. The two terms are comparable precisely in the crossover regime we have identified.

This idea leads to the conclusion that our main results found for the OU process are of more general validity. We explore this by considering the path of a Brownian particle in a general binding force field. Specifically, we consider  $U(x) = (1/\beta)(1 + x^2)^{\beta/2}$  with  $\beta > 0$ , which is symmetric around the origin and increases for large  $x$  as  $\propto x^\beta$ . In Fig. 4, we plot the mean  $\bar{z} = \langle z_{ds} \rangle$  versus  $T = \Delta N$  given various values of  $\beta$ . For the OU process with  $\beta = 2$ , we see that the numerical values converge to the IID limit at large times, see panel (a). This works

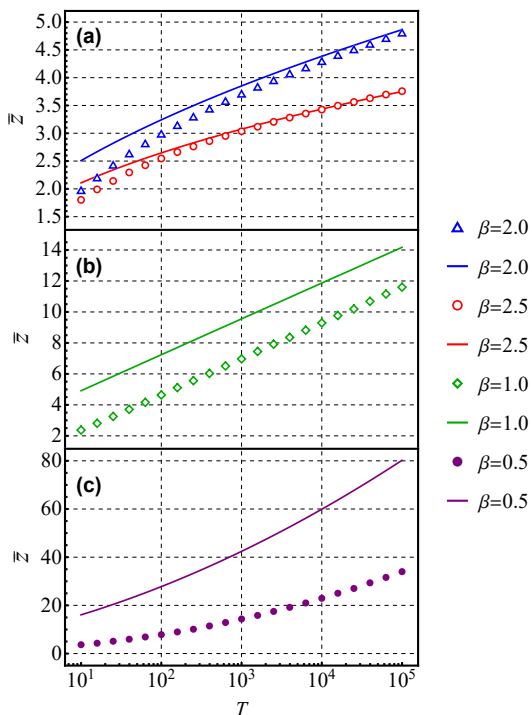


FIG. 4. (Color online) The mean EV  $\bar{z}$  of a correlated stochastic process  $x(t)$ , evolving via the Langevin equation, Eq. (1), with  $U(x) = (1/\beta)(1+x^2)^{\beta/2}$ . We used (a)  $\beta = 2$  and  $\beta = 5/2$  (marked by blue triangles and red circles), (b)  $\beta = 1$  (green diamonds), and (c)  $\beta = 1/2$  (purple disks), corresponding to the OU model, to an additional example of an increasing-force process, and to two counterexamples, a constant and a decreasing force, respectively. Seen are numerical evaluations for the four cases, where the sampling interval is  $\Delta = 0.1$ . Also depicted are the IID cases for each value of  $\beta$ , given by Eq. (2) (solid lines). For  $\beta > 1$ , the DS values converge to the IID description, see panel (a). The opposite happens for  $\beta < 1$ , as for this case the force vanishes for large distances, see panel (c). The borderline case is  $\beta = 1$ , where the DS and IID values do not seem to intersect, see panel (b). Each mean is made of  $10^4$  maxima whose initial conditions are  $x = 0$ , obtained using the Euler–Maruyama method with an underlying time increment of 0.01 (for  $\beta \neq 2$ ). Note that for  $\beta < 1$  we considered the semi-infinite case of  $x \in [0, z]$  instead [14].

also for  $\beta = 5/2$ , since here too the force grows with  $x$ , leading to a domination by the deterministic force term at long times. This argument is no longer valid for  $\beta \leq 1$ , where the force no longer increases with  $x$ , see panels (b) and (c). For example, when setting  $\beta = 1/2$ , the stochastic term dominates at large  $x$  and the exact values diverge from the IID behavior, see panel (c). Note that the critical case of  $\beta = 1$ , with an asymptotically constant force, is special, as here the numerical data is parallel to the IID limit, see panel (b).

Physically, the effect we find here is related to the fact that extreme events of Langevin paths in confining fields become larger as time progresses. However, the larger is the true maximum (in the CS sense), the faster the relax-

ation from this extreme gets, simply because the restoring force fields get enormously large if the path wanders to an EV. Here the value of  $\beta$  enters: If  $\beta > 1$  the forces are strong for extreme events, hence these are very short-lived and are more possible to be missed by DS, meaning that the DS and CS universality classes are not the same. Further, these strong fields effectively create uncorrelated RVs and indeed we have found the equilibrium density to control the EVs. In contrast, when the forces are asymptotically weaker, i.e.  $\beta < 1$ , the correlations are longer-lived, and the system is less sensitive to the size of the sampling interval. The asymptotically constant force of  $\beta = 1$  corresponds to an exponential distribution of the equilibrium measure, which is a special borderline case (this was shown to be true also for other problems, see Ref. [18] for example). Further analysis of the  $\beta \leq 1$  scenario is left for a future publication [14].

The support of Israel Science Foundation’s grant No. 1898/17 is acknowledged.

- 
- [1] E. J. Gumbel, *Statistics of Extremes* (Dover, New York 1958).
  - [2] M. R. Leadbetter, G. Lindgren, and H. Rootzen, *Extremes and Related Properties of Random Sequences and Processes* (Springer-Verlag, New York, 1982).
  - [3] F. Mori, S. N. Majumdar, and G. Schehr, arXiv:2104.07346 [cond-mat.stat-mech].
  - [4] Z. Schuss, K. Basnayake, and D. Holcman, *Phys. Life Rev.* **28**, 52 (2019).
  - [5] D. Sornette, L. Knopoff, Y. Y. Kagan, and C. Vanneste, *J. Geophys. Res.* **101**, 13883 (1996).
  - [6] P. Embrechts, C. Klüppelberg, and T. Mikosch, *Modelling Extremal Events for Insurance and Finance* (Springer, Berlin, 1997).
  - [7] L. H. C. Tippett and R. A. Fisher, *Proc. Cambridge Phil. Soc.* **24**, 180 (1928).
  - [8] B. V. Gnedenko, *Ann. Math.* **44**, 423 (1943).
  - [9] G. Györfgyi, N. R. Moloney, K. Ozogány, and Z. Rácz, *Phys. Rev. Lett.* **100**, 210601 (2008).
  - [10] O. Bénichou, P. L. Krapivsky, C. Mejía-Monasterio, and G. Oshanin, *Phys. Rev. Lett.* **117**, 080601 (2016).
  - [11] S. N. Majumdar, A. Pal, and G. Schehr, *Phys. Rep.* **840**, 1 (2020).
  - [12] D. S. Grebenkov, V. Sposini, R. Metzler, G. Oshanin, and F. Seno, *New J. Phys.* **23** 023014 (2021).
  - [13] L. Zarfaty, E. Barkai, and D. A. Kessler, *J. Phys. A: Math. Theor.* **54**, 315205 (2021).
  - [14] L. Zarfaty, E. Barkai, and D. A. Kessler, *In preparation*.
  - [15] Note that in Ref. [11], a typographical error resulted in an extra factor of two (S. N. Majumdar, private communication).
  - [16] Wolfram Research Inc., Mathematica, Version 12.1.1, Champaign, IL (2020).
  - [17] See the supplemental material for: I) The method used to numerically solve Eq. (4), and II) A derivation of Eqs. (7) and (8).
  - [18] S. Sabhapandit and S. N. Majumdar, *Phys. Rev. Lett.* **98**, 140201 (2007).

# Supplemental material for: Discrete sampling of extreme events modifies their statistics

Lior Zarfaty,<sup>1</sup> Eli Barkai,<sup>1</sup> and David A. Kessler<sup>2</sup>

<sup>1</sup>*Department of Physics, Institute of Nanotechnology and Advanced Materials, Bar-Ilan University, Ramat-Gan 52900, Israel*

<sup>2</sup>*Department of Physics, Bar-Ilan University, Ramat-Gan 52900, Israel*

In what follows, equations that are numbered without the prefix ‘‘SM’’ refer to their main text counterparts.

## THE METHOD USED TO NUMERICALLY SOLVE EQ. (4)

We start by splitting the integral in Eq. (4) as

$$\Lambda_*(z)P_*(x; z) = \int_{-\infty}^{x_m} dx' \frac{P_*(x'; z)}{\sqrt{2\pi(1-\mu^2)}} \exp\left[-\frac{(x-\mu x')^2}{2(1-\mu^2)}\right] + \int_{x_m}^z dx' \frac{P_*(x'; z)}{\sqrt{2\pi(1-\mu^2)}} \exp\left[-\frac{(x-\mu x')^2}{2(1-\mu^2)}\right], \quad (\text{SM1})$$

for some negative  $x_m$  with  $|x_m| \gg 1$ . Numerically, it proves useful to work with representations of the eigenfunction and eigenvalue that are based on the large- $z$  asymptotics (see next section below),

$$\tilde{P}_*(x; z) \equiv 1 - \frac{P_*(x; z)}{\phi(x)}, \quad \tilde{\Lambda}_*(z) \equiv 1 - \Lambda_*(z), \quad (\text{SM2})$$

where  $\phi(x) \equiv \exp(-z^2/2)/\sqrt{2\pi}$  is the standard Gaussian. Note that when  $z \rightarrow \infty$ , Eq. (4) can be solved in terms of  $P_*(x; z) = \phi(x)$  with  $\Lambda_*(z) = 1$ , and also that taking  $x \rightarrow -\infty$  has a similar mathematical consequence as taking  $z \rightarrow \infty$ . Thus, our next step is to express the eigenfunction as

$$\tilde{P}_*(x; z) \approx \begin{cases} \tilde{P}_n^*(x; z) & x_m \leq x \leq z \\ 0 & -\infty < x < x_m \end{cases}, \quad (\text{SM3})$$

where  $\tilde{P}_n^*(x; z)$  is the  $[x_m, z]$ -part of the eigenfunction corresponding to the  $n$ th iteration. Similarly, we denote  $\tilde{\Lambda}_n^*(z)$  as the  $n$ th iteration’s eigenvalue. Substituting Eq. (SM3) into Eq. (SM1), the latter’s first term can be computed explicitly, and we obtain

$$\tilde{\Lambda}_n^*(z) + \left[1 - \tilde{\Lambda}_n^*(z)\right] \tilde{P}_n^*(x; z) = \frac{1}{2} \operatorname{erfc}\left[\frac{z - \mu x}{\sqrt{2(1-\mu^2)}}\right] + \int_{x_m}^z dx' \frac{\tilde{P}_{n-1}^*(x'; z)}{\sqrt{2\pi(1-\mu^2)}} \exp\left[-\frac{(x' - \mu x)^2}{2(1-\mu^2)}\right] \quad (\text{SM4})$$

for  $x \in [x_m, z]$ . Then, assuming  $\tilde{P}_{n-1}^*(x; z)$  is known, we discretize  $x'$  on the interval  $[x_m, z]$  and perform the integral of Eq. (SM4). We find  $\tilde{\Lambda}_n^*(z)$  by evaluating Eq. (SM4) at  $x = x_m$ , where due to continuity  $\tilde{P}_n^*(x_m; z) = 0$ , yielding

$$\tilde{\Lambda}_n^*(z) = \frac{1}{2} \operatorname{erfc}\left[\frac{z - \mu x_m}{\sqrt{2(1-\mu^2)}}\right] + \int_{x_m}^z dx' \frac{\tilde{P}_{n-1}^*(x'; z)}{\sqrt{2\pi(1-\mu^2)}} \exp\left[-\frac{(x' - \mu x_m)^2}{2(1-\mu^2)}\right]. \quad (\text{SM5})$$

Using this value, we obtain  $\tilde{P}_n^*(x; z)$  for  $x \in [x_m, z]$ . Starting with  $\tilde{P}_0^*(x; z) = 0$  and continuing to iterate gives a series of approximations to  $\tilde{P}_*(x; z)$  which converges efficiently. We define a measure of convergence to determine the stopping point of this iterative process,

$$\tilde{\mathcal{E}} \equiv \left| \frac{\tilde{\Lambda}_{100m}^*(z)}{\tilde{\Lambda}_{100(m-1)}^*(z)} - 1 \right|, \quad 1 < m \in \mathbb{N}. \quad (\text{SM6})$$

This prescription was used to obtain the numerical data for  $\Lambda_*(z)$  presented in Figs. 2 and 3. We used  $x_m = -5$ ,  $\mathcal{E} = 10^{-7}$ , and the discretization step in  $x$  was 0.01.

**DERIVATION OF EQS. (7) AND (8)**

We start by writing that for large- $z$

$$P_*(x; z) \simeq \phi(x) \left[ 1 + e^{-z^2/2} \mathcal{P}_1(x; z) + e^{-z^2} \mathcal{P}_2(x; z) \right], \quad \Lambda_*(z) \simeq 1 + e^{-z^2/2} \Lambda_1(z) + e^{-z^2} \Lambda_2(z). \quad (\text{SM7})$$

These expansions are to be understood in the context of a fixed  $\mu < 1$ . Plugging the above expansion into Eq. (4), we get to first order

$$\phi(x) \left[ 1 + e^{-z^2/2} \mathcal{P}_1(x; z) + e^{-z^2} \Lambda_1(z) \right] = \int_{-\infty}^z dx' \phi(x') \frac{1 + e^{-z^2/2} \mathcal{P}_1(x'; z)}{\sqrt{2\pi(1-\mu^2)}} \exp \left[ -\frac{(x - \mu x')^2}{2(1-\mu^2)} \right]. \quad (\text{SM8})$$

The zeroth-order equation is satisfied since

$$\int_{-\infty}^z dx' \phi(x') \frac{1}{\sqrt{2\pi(1-\mu^2)}} \exp \left[ -\frac{(x - \mu x')^2}{2(1-\mu^2)} \right] = \phi(x) \left\{ 1 - \frac{1}{2} \operatorname{erfc} \left[ \frac{z - x\mu}{\sqrt{2(1-\mu^2)}} \right] \right\}, \quad (\text{SM9})$$

where  $\operatorname{erfc}(\cdot)$  is the complementary error function. Using the following expansion [1] of the Gaussian kernel function of Eq. (4), which holds for  $0 \leq \mu < 1$ ,

$$\frac{1}{\sqrt{2\pi(1-\mu^2)}} \exp \left[ -\frac{(x - \mu x')^2}{2(1-\mu^2)} \right] = \phi(x) \sum_{n=0}^{\infty} \frac{\mu^n}{n!} \operatorname{He}_n(x) \operatorname{He}_n(x'), \quad (\text{SM10})$$

where  $\operatorname{He}_n(\cdot)$  is the  $n$ th probabilist's Hermite polynomial, we obtain to first order

$$\mathcal{P}_1(x; z) + \Lambda_1(z) + \frac{1}{2} e^{z^2/2} \operatorname{erfc} \left[ \frac{z - x\mu}{\sqrt{2(1-\mu^2)}} \right] - \int_{-\infty}^{\infty} dx' \phi(x') \mathcal{P}_1(x'; z) \sum_{n=0}^{\infty} \frac{\mu^n}{n!} \operatorname{He}_n(x) \operatorname{He}_n(x') = 0. \quad (\text{SM11})$$

Note that we have extended the integral's boundary to infinity, dropping a higher-order correction to be accounted for during the second-order calculation. Exploiting another expansion [2] similar to the one above,

$$\operatorname{erfc} \left[ \frac{z - x\mu}{\sqrt{2(1-\mu^2)}} \right] = \operatorname{erfc} \left( \frac{z}{\sqrt{2}} \right) + 2\phi(z) \sum_{n=1}^{\infty} \frac{\mu^n}{n!} \operatorname{He}_n(x) \operatorname{He}_{n-1}(z), \quad (\text{SM12})$$

together with expressing the first functional correction as a sum over Hermite polynomials in  $x$ ,

$$\mathcal{P}_1(x; z) = \sum_{n=0}^{\infty} c_n(z) \operatorname{He}_n(x), \quad (\text{SM13})$$

and using their orthogonality condition (where  $\delta_{n,m}$  is the Kronecker delta),

$$\int_{-\infty}^{\infty} dx' \phi(x') \operatorname{He}_n(x') \operatorname{He}_m(x') = \delta_{n,m} n!, \quad (\text{SM14})$$

we get for the first-order expansion

$$\left[ c_0(z) (1 - \mu^0) + \Lambda_1(z) + \frac{1}{2} e^{z^2/2} \operatorname{erfc} \left( \frac{z}{\sqrt{2}} \right) \right] \operatorname{He}_0(x) + \sum_{n=1}^{\infty} \left[ c_n(z) (1 - \mu^n) + \frac{\mu^n/n!}{\sqrt{2\pi}} \operatorname{He}_{n-1}(z) \right] \operatorname{He}_n(x) = 0. \quad (\text{SM15})$$

Thus, we obtain

$$\Lambda_1(z) = -\frac{1}{2} e^{z^2/2} \operatorname{erfc} \left( \frac{z}{\sqrt{2}} \right), \quad c_n(z) = -\frac{\mu^n/n!}{\sqrt{2\pi}} \frac{\operatorname{He}_{n-1}(z)}{1 - \mu^n}, \quad n > 0. \quad (\text{SM16})$$

The value of  $c_0(z)$  can be found from the condition  $\mathcal{P}_1(0; z) = 0$ , since an  $x$ -independent addition to  $\mathcal{P}_1(x; z)$  is just a change of normalization. This yields

$$c_0(z) = -\sum_{n=1}^{\infty} c_n(z) \operatorname{He}_n(0) = -\sum_{n=1}^{\infty} \frac{\sqrt{\pi} 2^{n/2} c_n(z)}{\Gamma[(1-n)/2]}, \quad (\text{SM17})$$

where  $\Gamma(\cdot)$  is the gamma function.

Since we have an exact solution of the first-order equation, we can move on to the second order. We further expand Eq. (4) to second-order, obtaining

$$\begin{aligned} \mathcal{P}_2(x; z) + \mathcal{P}_1(x; z)\Lambda_1(z) + \Lambda_2(z) + e^{z^2/2} \int_z^\infty dx' \phi(x') \mathcal{P}_1(x'; z) \sum_{n=0}^\infty \frac{\mu^n}{n!} \text{He}_n(x) \text{He}_n(x') \\ - \int_{-\infty}^\infty dx' \phi(x') \mathcal{P}_2(x'; z) \sum_{n=0}^\infty \frac{\mu^n}{n!} \text{He}_n(x) \text{He}_n(x') = 0. \end{aligned} \quad (\text{SM18})$$

The first integral term is the higher-order correction that was dropped in Eq. (SM11). As was done above, the boundary of the second integral term was extended to infinity (as the contribution from  $x' \in [z, \infty)$  only enters the calculation of the third-order correction). Expressing  $\mathcal{P}_2(x; z)$  similarly to its first-order counterpart,

$$\mathcal{P}_2(x; z) = \sum_{n=0}^\infty d_n(z) \text{He}_n(x), \quad (\text{SM19})$$

and rearranging the terms, we get

$$\Lambda_2(z) = \sum_{n=1}^\infty \frac{\mu^n/n!}{1-\mu^n} \phi_{n,0}(z) \text{He}_{n-1}(z), \quad (\text{SM20})$$

with [3]

$$\phi_{n,m}(z) \equiv \frac{e^{z^2/2}}{\sqrt{2\pi}} \int_z^\infty dx \phi(x) \text{He}_n(x) \text{He}_m(x) = \frac{1}{2\pi} \sum_{l=0}^L l! \binom{n}{l} \binom{m}{l} \text{He}_{n+m-2l-1}(z) + \delta_{n,m} \frac{n!/2}{\sqrt{2\pi}} e^{z^2/2} \text{erfc}\left(\frac{z}{\sqrt{2}}\right), \quad (\text{SM21})$$

where  $L \equiv \min(n, m) - \delta_{n,m}$  and we used the standard convention that a summation from 0 to  $-1$  vanishes. Taking  $m = 0$  and  $n \geq 1$ , we get  $\phi_{n,0}(z) = (1/2\pi) \text{He}_{n-1}(z)$ , hence

$$\Lambda_2(z) = \frac{1}{2\pi} \sum_{n=1}^\infty \frac{\mu^n/n!}{1-\mu^n} \text{He}_{n-1}^2(z), \quad (\text{SM22})$$

which, together with  $\Lambda_1(z)$  from Eq. (SM16), yields Eq. (7) when plugged into Eq. (SM7). Finally, using the identity

$$\sum_{n=0}^\infty \frac{\nu^n}{n!} \text{He}_n^2(z) = \frac{1}{\sqrt{1-\nu^2}} \exp\left(\frac{z^2\nu}{1+\nu}\right), \quad (\text{SM23})$$

which arises in the calculation of the density of states of the finite temperature quantum harmonic oscillator [4], we find

$$\Lambda_2(z) = \frac{1}{2\pi} \sum_{n=1}^\infty \int_0^{\mu^n} \frac{d\nu}{\sqrt{1-\nu^2}} \exp\left(\frac{z^2\nu}{1+\nu}\right) \underset{z \rightarrow \infty}{\sim} \frac{(1+\mu)^2}{\sqrt{1-\mu^2}} \frac{1}{2\pi z^2} \exp\left(\frac{z^2\mu}{1+\mu}\right), \quad (\text{SM24})$$

where the latter part of it, together with expanding  $\Lambda_1(z)$  for  $z \rightarrow \infty$ , yields Eq. (8).

---

[1] See [functions.wolfram.com/05.01.23.0013.01](http://functions.wolfram.com/05.01.23.0013.01) with  $z = x/\sqrt{2}$ ,  $z_1 = x'/\sqrt{2}$ , and  $w = \mu/2$ .

[2] One can prove Eq. (SM12) by differentiating it with respect to  $\mu$ , and using  $\text{He}_n(x) = x\text{He}_{n-1}(x) - \text{He}'_{n-1}(x)$  together with Eq. (SM10) to show that the resulted expression holds. Verifying that Eq. (SM12) is satisfied for  $\mu = 0$  concludes the proof.

[3] Equation (SM21) can be proved by a differentiation with respect to  $z$ , followed by exploiting  $\text{He}_n(x) = x\text{He}_{n-1}(x) - \text{He}'_{n-1}(x)$  together with the identity <http://functions.wolfram.com/05.01.16.0006.01> to verify that the resulted expression is satisfied. Showing that Eq. (SM21) holds for  $z \rightarrow -\infty$  concludes the proof.

[4] B. V. Bondarev, *App. Math.* **8**, 1529-1538 (2017).